Electronic Supplementary Information

Rechargeable Aqueous Zinc-iodine Batteries: Pore Confining Mechanism and Flexible Device Application

Yixin Li, Luojia Liu, Haixia Li, Fangyi Cheng and Jun Chen*

Key Laboratory of Advanced Energy Materials Chemistry (Ministry of Education), College of Chemistry, Nankai University, Tianjin 300071, China

Corresponding Author

* E-mail: fycheng@nankai.edu.cn

Experimental section

Preparation of iodine/carbon cloth and iodine/CMK-3

The iodine/carbon cloth was prepared by a previously reported room-temperature "solution-adsorption" process.[1] In a typical example, 100 mg iodine was added into 200 ml distilled water and 10 cm^2 carbon cloth was loaded. After stirring for about 12 h, the iodine undissolved in water was absorbed effectively and the solution turned clear. The prepared iodine/carbon cloth (8.8 mg/cm^2 iodine loading) was dried in an air-circulating oven at 60 °C. The amount of absorbed iodine was calculated according to the mass difference before and after adsorbing iodine. Iodine/carbon cloths with different iodine loadings of 3.2, 6.7 and 12.4 mg cm^{-2} were prepared through similar procedure. The iodine/CMK-3 composite was prepared via procedures similar to that for the iodine/carbon cloth. Typically, 100 mg iodine and 80 mg CMK-3 were added into 200 ml distilled water. After stirring for about 12 h, the formed mixture was filtered to obtain iodine/CMK-3, which was finally dried in oven at 60 °C.

Characterization of iodine /carbon cloth

SEM (JEOL JSM7500F) and TEM (Philips Tecnai G2F-20) were used to observe the morphology of pure carbon cloth and the as-prepared iodine/carbon cloth. Brunauer-Emmett-Teller (BET) surface areas were measured with a BEL Sorp-Mini instrument using N_2 adsorption-desorption at 77 K. The crystallinity of iodine, carbon cloth and iodine/carbon cloth was characterized by X-ray diffraction (XRD, Rigaku MiniFlex600, Cu). The elemental information and the surface chemical composition were measured by X-ray photoelectron spectrometry (XPS, Perkin Elmer PHI 1600 ESCA). Ex-situ UV-Vis spectra (Jasco V-550) and in-situ Raman spectra (collected on Thermo DXR at 532 nm excitation) were measured to investigate the reaction mechanism.

DFT calculations of Zn-iodine, Li-iodine and Na-iodine batteries

DFT calculations were performed using Gaussian 09W A.02 software packages with the 3-parameter hybrid Becke exchange/Lee-Yang-Parr correlation functional level of theory.[2] Basis set 6-31+G (d, p) was applied to Li and Na atoms, while Zn and I adopted lanl2dz basis sets for better description of relativistic effect.

Fabrication of Zn-iodine batteries

Both the coin-type and cable type Zn-iodine/carbon cloth batteries were assembled with Nafion 117 membrane as the separator and 2 M $ZnSO_4$ as the electrolyte. The coin cells were assembled using a zinc foil as the anode and the as-prepared iodine/carbon cloth cut into wafer (10 mm diameter) as the cathode. To make the cable-type Zn-iodine batteries, the iodine/carbon cloth was cut into a 0.5×4 cm^2 cathode to couple with a zinc wire anode. After twisting the as-prepared cathode and a Nafion membrane (0.5 cm width, 6 cm length) on the surface of the zinc wire, the electrodes and membrane were sealed by a heat-contraction rubber cable. Finally, the electrolyte was injected by a peristaltic pump tardily, followed by heating the rubber cable in 100 °C oven within 5 min. The coin-type Zn-iodine/KS6 and Zn-iodine/Super P batteries were assembled using filter paper as separator to observe the colour change during the discharge process. Pristine iodine/KS6 and iodine/Super P electrodes were prepared by mixing I_2 (40 wt%), conductive carbon materials (KS6 or Super P, respectively, 50 wt%), CMC binder (10 wt%) and deionized water as dispersing agent to form slurries, which were separately smeared onto a Ti foil current collector (cut into 10 mm diameter wafer) and dried at room temperature for battery assembly. Coin-type Zn-iodine/CMK-3 battery was assembled using Nafion membrane as the separator for electrochemical testing. The cathode was composed of 80 wt% iodine/CMK-3, 10 wt% super P and 10 wt% CMC.

Electrochemical Measurements of Zn-iodine batteries

A LAND-CT2001A battery testing instrument was applied for galvanostatic charge/discharge tests in the voltage range of 0.5–1.8 V. Cyclic voltammograms (CVs) were performed on a PARSTAT electrochemical workstation (CHI660E) at the scan rates of 0.1 mV s^{-1} in the potential window of 0.5–1.8 V.

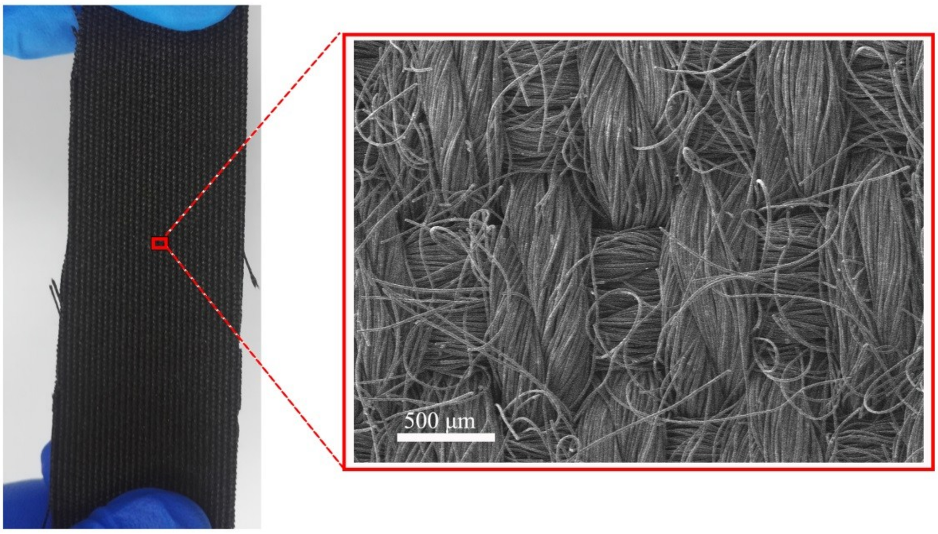

Fig. S1 The digital photograph and SEM image of pristine carbon cloth.

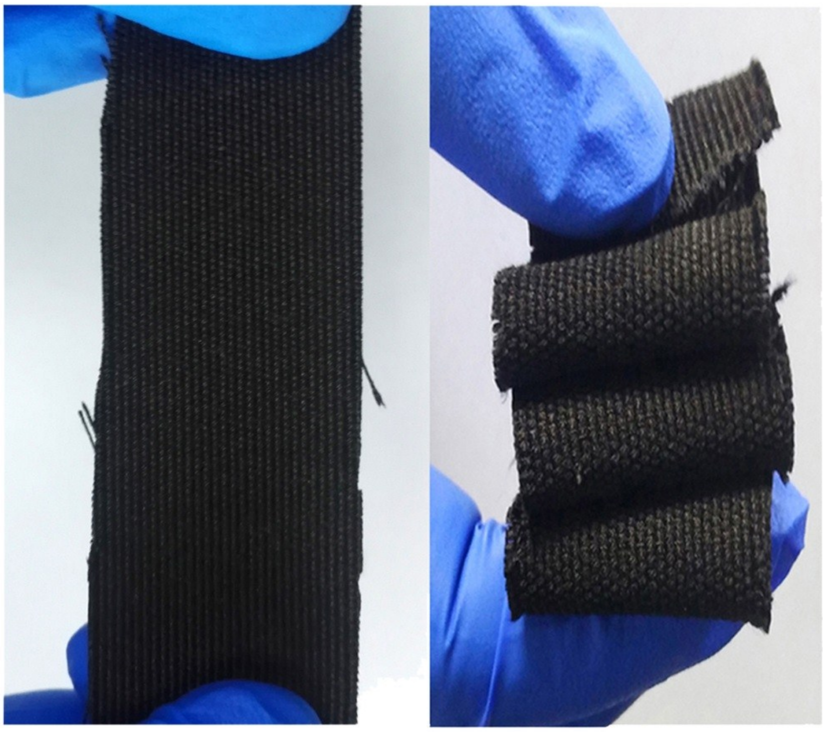

Fig. S2 The digital photographs of iodine/carbon cloth.

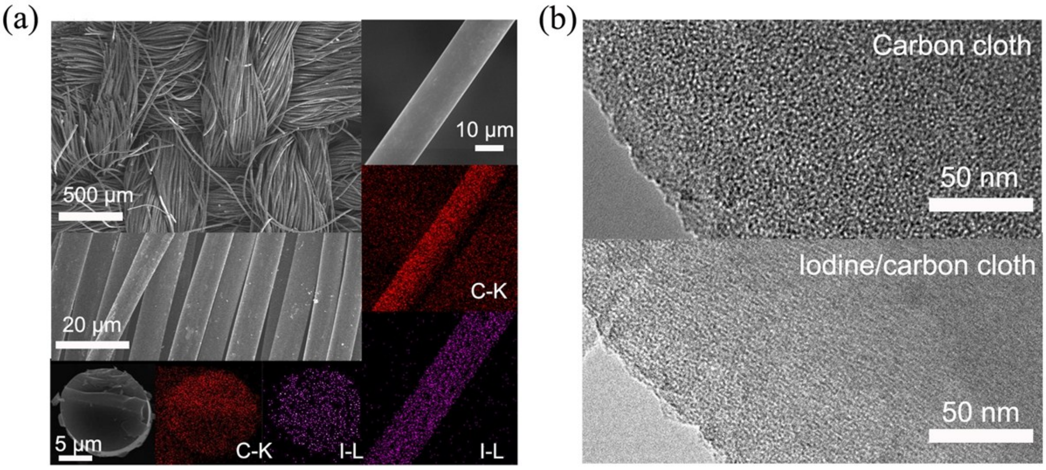

Fig. S3 (a) SEM images and elemental mapping from side and cross-section views. (b) TEM images of pristine carbon cloth and iodine/carbon cloth

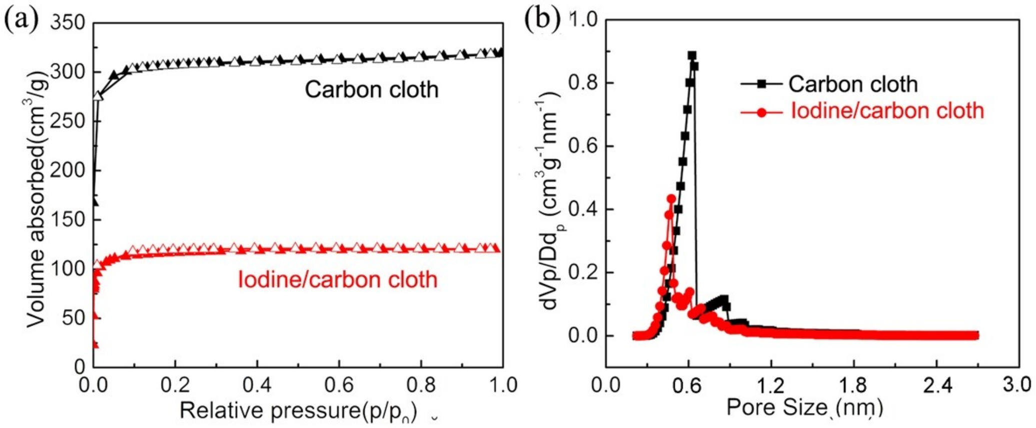

Fig. S4 (a)N_2 adsorption-desorption isotherms and (b) Pore size distribution of carbon cloth and iodine/carbon cloth. The pristine carbon cloth features large specific surface area (1225.8 m^2 g^{-1}) and typical microporous structure with pore size of 0.63 nm. As expected, filling iodine inside the pores of carbon fibers resulted in a dramatic decrease of the specific surface area and pore size.

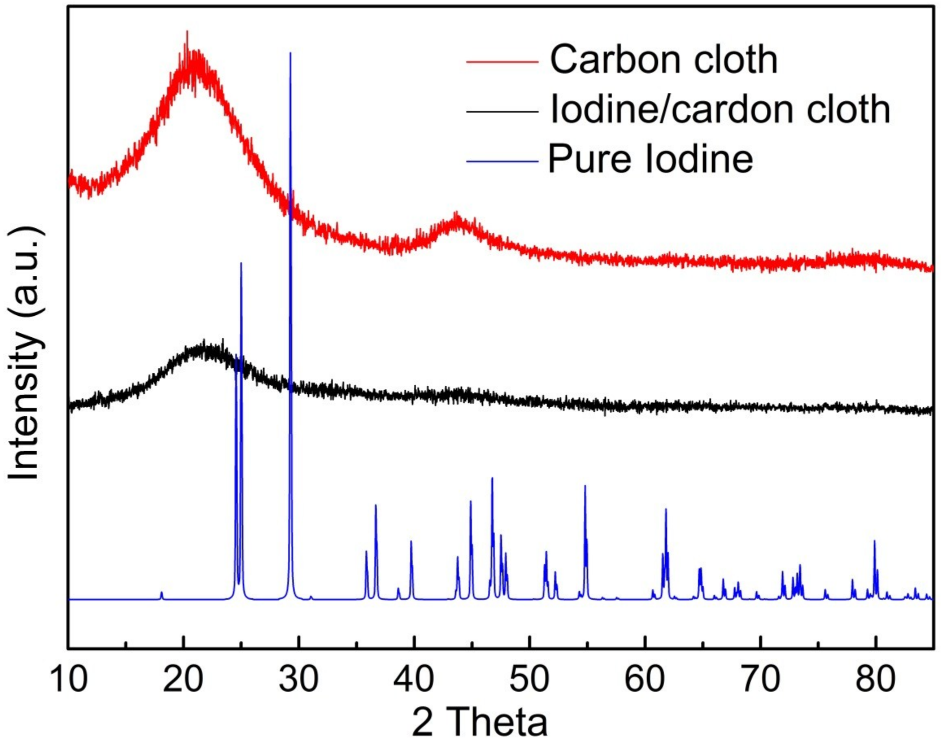

Fig. S5 XRD patterns of pure iodine, pristine carbon cloth and iodine/carbon cloth.

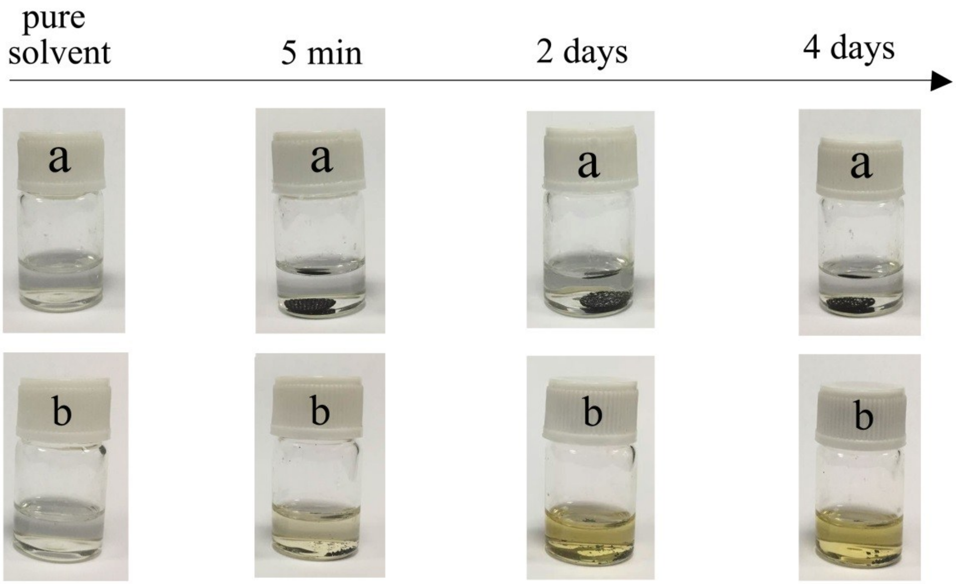

Fig. S6 Solubility test of (a) iodine/carbon cloth and (b) pure iodine. 6.8 mg iodine on carbon cloth (a) and 6.8 mg iodine powder (b) were separately added into a 2 mL of 2 M $ZnSO_4$ solution. Without the absorption of carbon cloth, the iodine was rapidly dissolved in electrolyte, with the color of solution turning yellow gradually. After being adsorbed by carbon cloth, the dissolved iodine was largely trapped with iodine/carbon cloth, showing no obvious color change after 4 days.

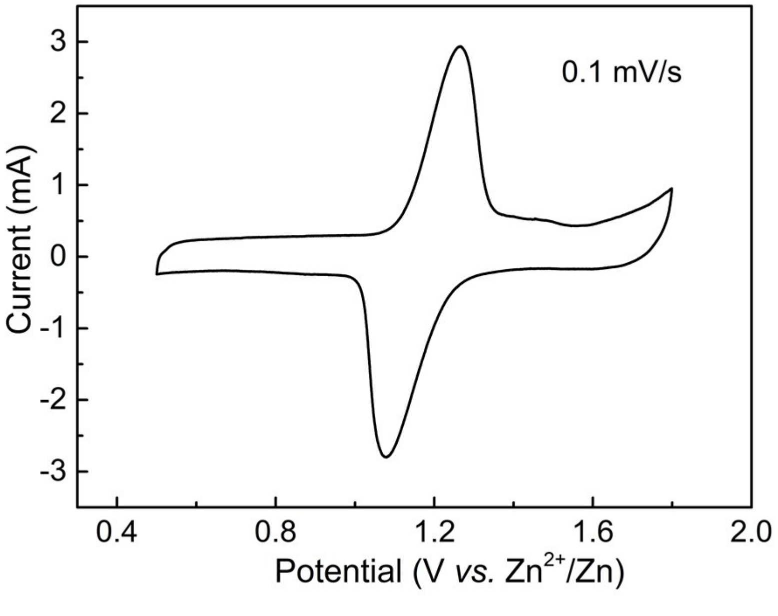

Fig. S7 Cyclic voltammetry of iodine/carbon cloth electrodes.

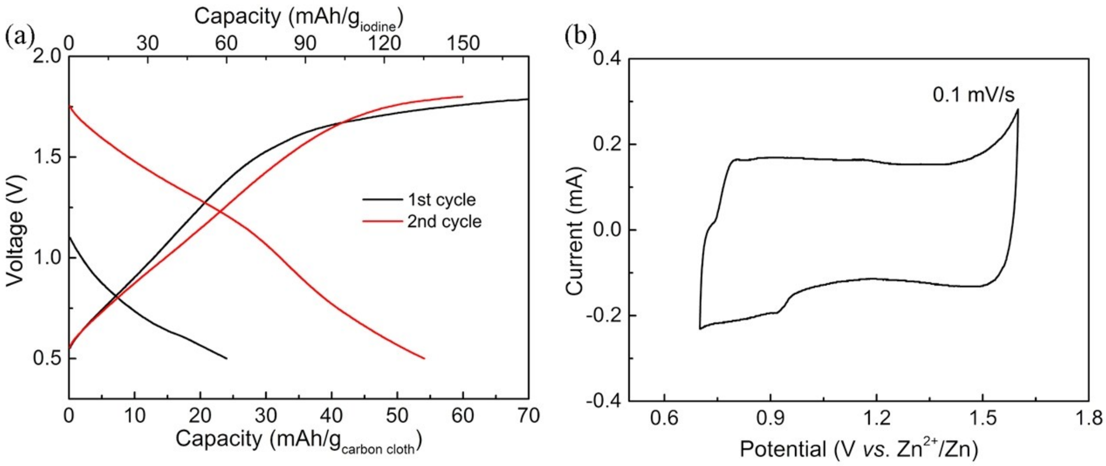

Fig. S8 (a) Discharge and charge curves of neat carbon cloth at the first and second cycles at the current density of 1 mA cm^{-2}. (b) Cyclic voltammetry of neat carbon cloth electrode. The neat carbon cloth substrate shows a typical capacitance behavior, as seen from the shape of the CV curve. At the first cycle, the neat carbon cloth contributes to a lower capacity due to low voltage. After that, the neat carbon cloth delivers a capacity of 53 mAh g^{-1} (based on the mass of carbon), corresponding to 135 mAh g^{-1} based on the mass of iodine (iodine loading of 8.8 mg cm^{-2}).

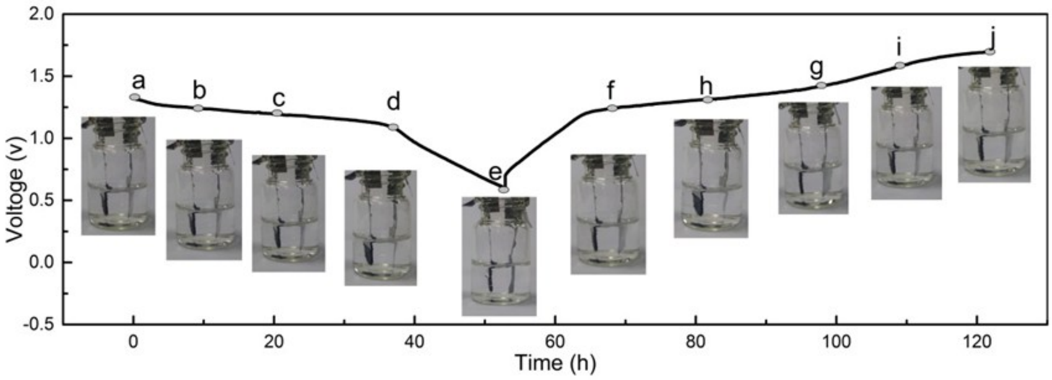

Fig. S9 Visual images of the discharge and charge process of a Zn-iodine/carbon cloth battery at different states.

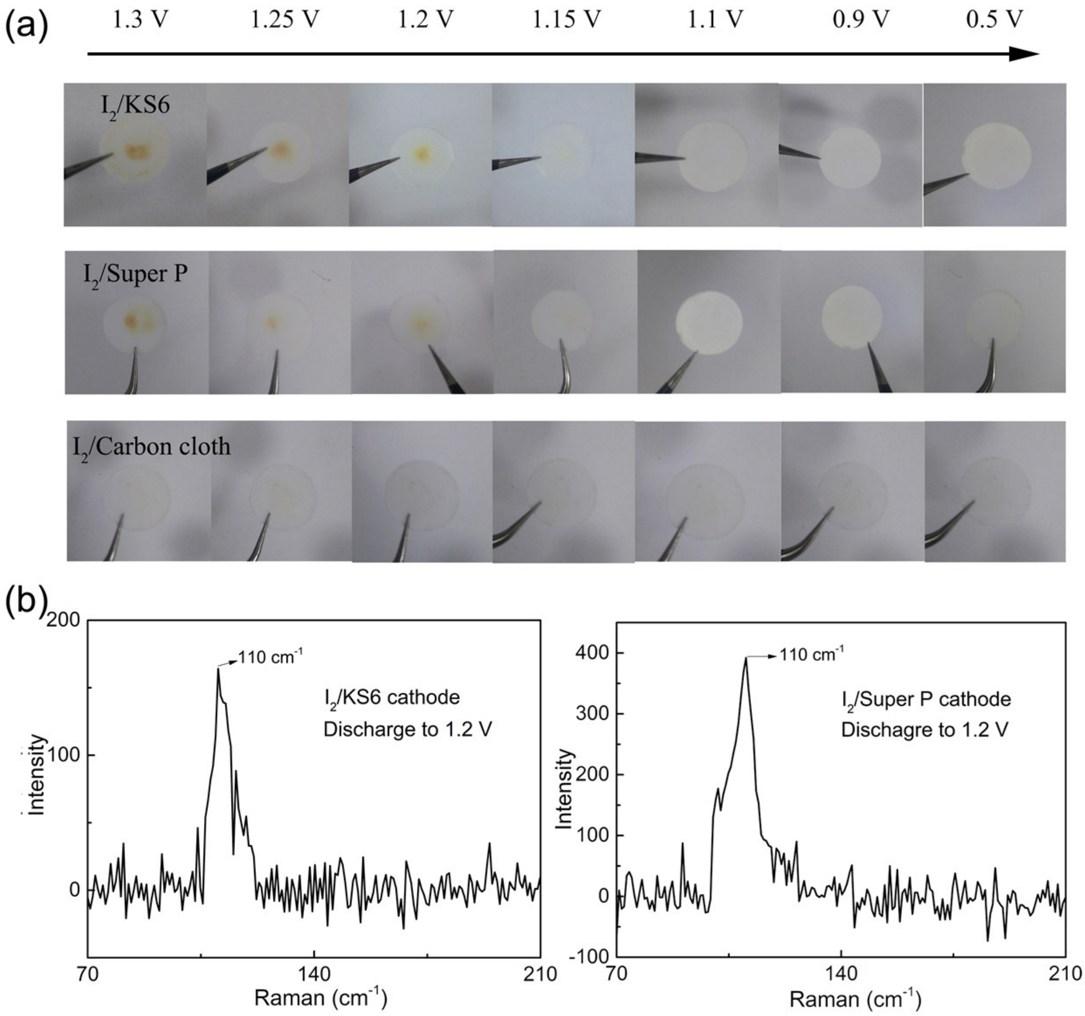

Fig. S10 (a) Digital photos of the separators of Zn-iodine battery with conductive graphite powder KS6, conductive carbon Super P and carbon cloth as cathodes. (b) Raman analysis of the discharged (discharge to 1.2 V) I_2/KS6 and I_2/Super P cathode. Compared with the nonporous KS6 and Super P, the Zn-iodine/carbon cloth showed no visible change in color during the discharge progress. However, on discharging from 1.3 to 1.2 V, the separators of Zn-I_2/KS6 and Zn-I_2/Super P turned deep yellow, indicating the formation of I_3^-. Raman analysis of the discharged cathodes further indicated the formation of I_3^-.

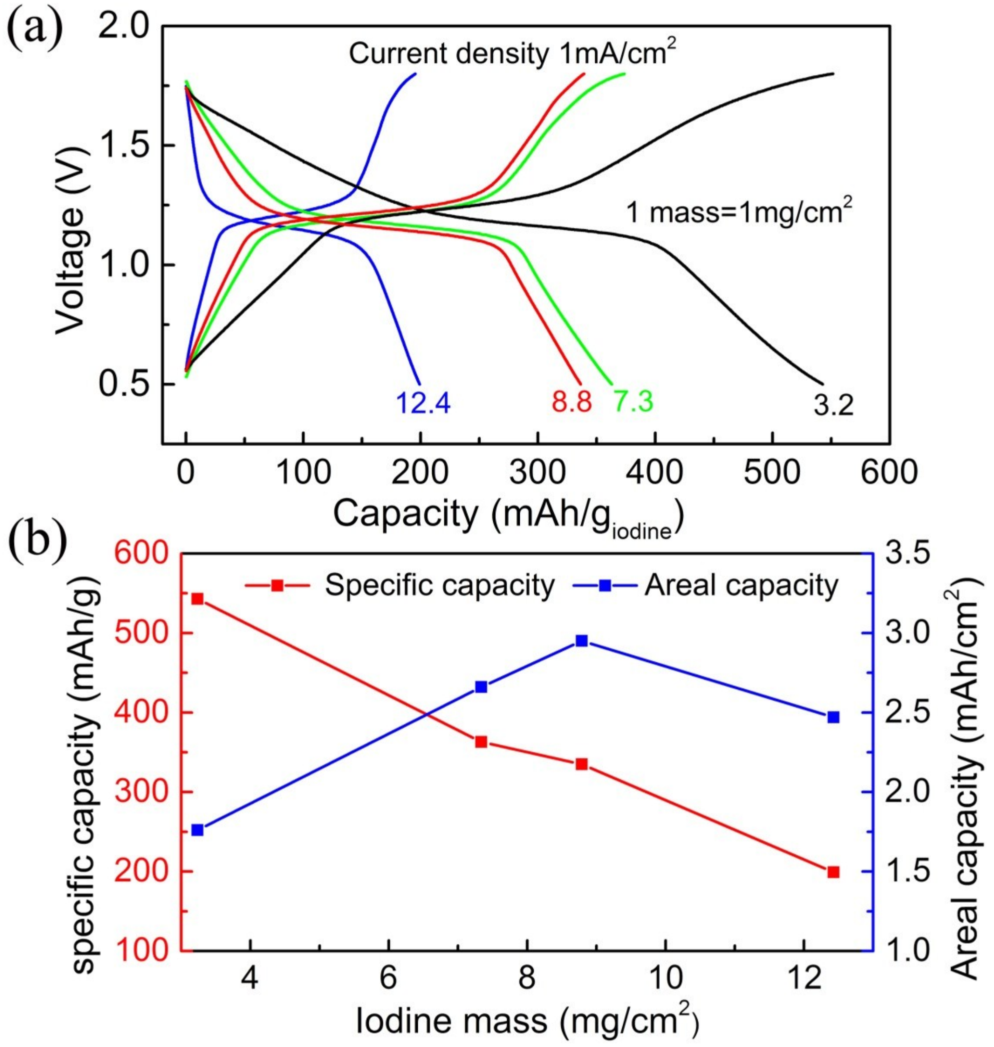

Fig. S11 (a) Initial discharge and charge curves of cathodes with different iodine mass at current density of 1 mA/cm^2. (b) Corresponding initial discharge capacity based on mass and area.

Table S1 Comparison of the electrochemical performance of different iodine/carbon cloth cathodes at a current density of 1 mA/cm^2 (all capacities were calculated by the mass of iodine).

Iodine loading	**Total capacity**	**Capacity contributed**	**Total specific**	**Specific capacity**	**Utilization efficiency of**

(mg/cm^2)	**(mAh)**	**by iodine (mAh)**	**capacity (mAh/g)**	**contributed by iodine (mAh/g)**	**iodine**
0	0.93	0	---	---	---
3.236	1.38	0.45	543	177	84%
7.337	2.09	1.16	363	201	95%
8.789	2.31	1.38	335	200	95%
12.430	1.94	1.01	199	103	50%

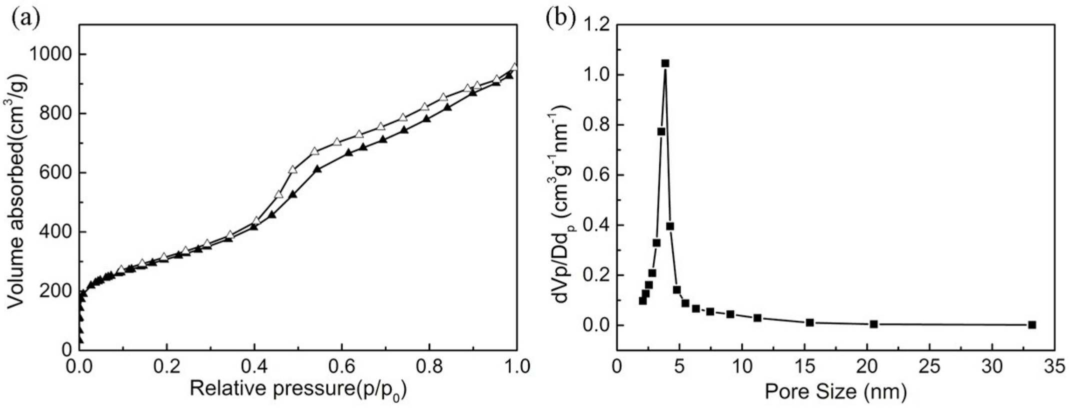

Fig. S12 (a) N_2 adsorption-desorption isotherms and (b) Pore size distribution of CMK-3.

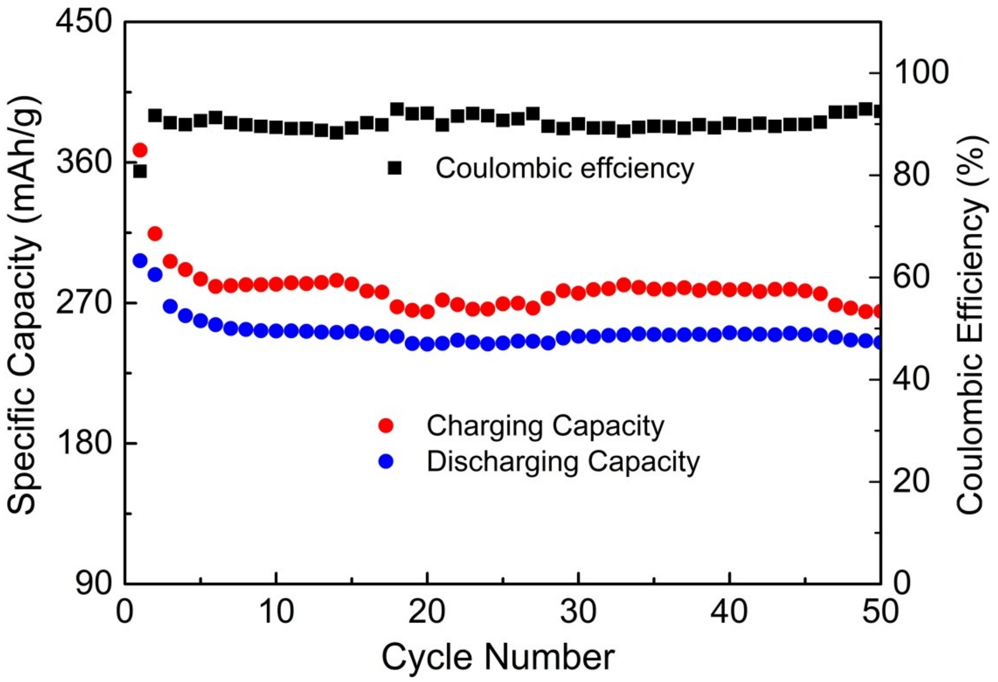

Fig. S13 Cycling performance of iodine/CMK-3 electrodes at 1 mA cm^{-2}.

References

1. Q. Zhao, Y. Lu, Z. Zhu, Z. Tao and J. Chen, Nano Lett., 2015, 15, 5982.
2. M. J. Frisch, G. W. Trucks, H. B. Schlegel, G. E. Scuseria, M. A. Robb, J. R. Cheeseman, J. A. Montgomery Jr., T. Vreven, K. N. Kudin, J. C. Burant, J. M. Millam, S. S. Iyengar, J. Tomasi, V. Barone, B. Mennucci, M. Cossi, G. Scalmani, N. Rega, G. A. Petersson, H. Nakatsuji, M. Hada, M. Ehara, K. Toyota, R. Fukuda, J. Hasegawa, M. Ishida, T. Nakajima, Y. Honda, O. Kitao, H. Nakai, M. Klene, X. Li, J. E. Knox, H. P. Hratchian, J. B. Cross, V. Bakken, C. Adamo, J. Jaramillo, R. Gomperts, R. E. Stratmann, O. Yazyev, A. J. Austin, R. Cammi, C. Pomelli, J. W. Ochterski, P. Y. Ayala, K. Morokuma, G. A. Voth, P. Salvador, J. J. Dannenberg, V. G. Zakrzewski, S. Dapprich, A. D. Daniels, M. C. Strain, O. Farkas, D. K.

Malick, A. D. Rabuck, K. Raghavachari, J. B. Foresman, J. V. Ortiz, Q. Cui, A. G. Baboul, S. Clifford, J. Cioslowski, B. B. Stefanov, G. Liu, A. Liashenko, P. Piskorz, I. Komaromi, R. L. Martin, D. J. Fox, T. Keith, M. A. Al-Laham, C. Y. Peng, A. Nanayakkara, M. Challacombe, P. M. W. Gill, B. Johnson, W. Chen, M. W. Wong, C. Gonzalez, J. A. Pople, Gaussian 09, Revision A.02, Gaussian, INC., Wallingford, CT, 2009.